

## Detection of urinary microRNA biomarkers using diazo sulfonamide-modified screen printed carbon electrodes†

### Electronic supplementary information

Daniel A. Smith<sup>a,b</sup>, Kate Simpson<sup>a</sup>, Matteo Lo-Cicero<sup>c</sup>, Lucy J. Newbury<sup>a,b</sup>, Philip Nicholas<sup>d</sup>, Donald J. Fraser<sup>a,b</sup>, Nigel Caiger<sup>d</sup>, James E. Redman<sup>b,c,1</sup>, Timothy Bowen<sup>a,b,\*,1</sup>

<sup>a</sup> Wales Kidney Research Unit, Division of Infection & Immunity, School of Medicine, College of Biomedical and Life Sciences, Cardiff University, Heath Park, Cardiff CF14 4XN, UK. E-mail: bowent@cf.ac.uk

<sup>b</sup> Cardiff Institute of Tissue Engineering and Repair, Museum Place, Cardiff CF10 3BG, UK

<sup>c</sup> School of Chemistry, College of Physical Sciences and Engineering, Cardiff University, Cardiff CF10 3AT, UK

<sup>d</sup> Sun Chemical Ltd, Midsomer Norton, Radstock, Bath BA3 4RT, UK

<sup>1</sup> These authors contributed equally to this work.

\*Corresponding author

### Table of Contents

<b>Figure S1: Oligonucleotides used in the study. ....</b>	<b>2</b>
<b>Figure S2: CV changes over fabrication steps.....</b>	<b>2</b>
<b>Figure S3: Reductive coulometry changes over fabrication steps.....</b>	<b>3</b>
<b>Figure S4: Oxidative coulometry changes over fabrication steps. ....</b>	<b>3</b>
<b>Figure S5: CV deposition cycles. ....</b>	<b>4</b>
<b>Figure S6: Example oxidative coulometry response following hybridisation with decreasing concentrations of miR-21. ....</b>	<b>4</b>
<b>Figure S7: Oxidative coulometry calibration plot for miR-21. Data are expressed as mean +/- SEM. 5</b>	<b>5</b>
<b>Figure S8: Example differential pulse voltammetry (DPV) response following hybridisation with decreasing concentrations of miR-21. ....</b>	<b>5</b>
<b>Figure S9: Differential pulse voltammetry (DPV) calibration plot for miR-21. Data are expressed as mean +/- SEM. ....</b>	<b>6</b>
<b>Figure S10: Oxidative coulometry (Echem) and RT-qPCR (PCR) analysis of urinary miR-192 in DKD patients and control subjects. Data were normalised to miR-191 and are expressed as mean as +/- SEM (n = 6 each group). * = P &lt; 0.05. ....</b>	<b>6</b>
<b>Figure S11: Reductive coulometry analysis of miR-21 in serial dilutions (1/10<sup>th</sup>, 1/50<sup>th</sup>, 1/100<sup>th</sup>, 1/500<sup>th</sup>, 1/1000<sup>th</sup>, 1/5000<sup>th</sup>) of control urine following proteinase K treatment. Data are expressed as mean +/- SEM (n = 3). ....</b>	<b>7</b>
<b>Figure S12: Reductive coulometry measurements investigating uric acid interference, uric acid solutions without microRNA in blue followed by addition of 10<sup>-11</sup> M miR-21. Data are expressed as means +/- SEM (n = 3). ....</b>	<b>7</b>
<b>Figure S13: Oxidative coulometry measurements investigating uric acid interference, uric acid solutions without microRNA in blue followed by addition of 10<sup>-11</sup> M miR-21. Data are expressed as means +/- SEM (n = 3). ....</b>	<b>8</b>
<b>Figure S14: Additional AFM images captured during SPCE modification. ....</b>	<b>9</b>

Figure S1: Oligonucleotides used in the study.

<u>Oligonucleotide Name</u>	<u>Oligonucleotide Sequence</u>
<i>comp-miR-21 (DNA)</i>	5'NH <sub>2</sub> -C <sub>6</sub> -TCA ACA TCA GTC TGA TAA GCT A
<i>miR-21 (RNA)</i>	5' -UAG CUU AUC AGA CUG AUG UUG A
<i>comp-miR-192 (DNA)</i>	5'NH <sub>2</sub> -C <sub>6</sub> -GGC TGT CAA TTG ATA GGT CAG
<i>miR-192 (RNA)</i>	5' -CUG ACC UAU GAA UUG ACA GCC
<i>comp-miR-191 (DNA)</i>	5'NH <sub>2</sub> -C <sub>6</sub> -CAG CTG CTT TTG GGA TTC CGT TG
<i>miR-191 (RNA)</i>	5' -CAA CGG AAU CCC AAA AGC AGC UG
<i>comp-miR-223 (DNA)</i>	5'NH <sub>2</sub> -C <sub>6</sub> -TGG GGT ATT TGA CAA ACT GAC A
<i>miR-16 (RNA)</i>	5' -UAG CAG CAC GUA AAU AUU GGC G
<i>3'-bio-comp-miR-21 (DNA)</i>	5'NH <sub>2</sub> -C <sub>6</sub> -TCA ACA TCA GTC TGA TAA GCT A-Biotin
<i>5'-bio-miR-21 (RNA)</i>	5' Biotin-UAG CUU AUC AGA CUG AUG UUG A

\*Comp = complementary, bio = biotin label.

Figure S2: CV changes over fabrication steps.

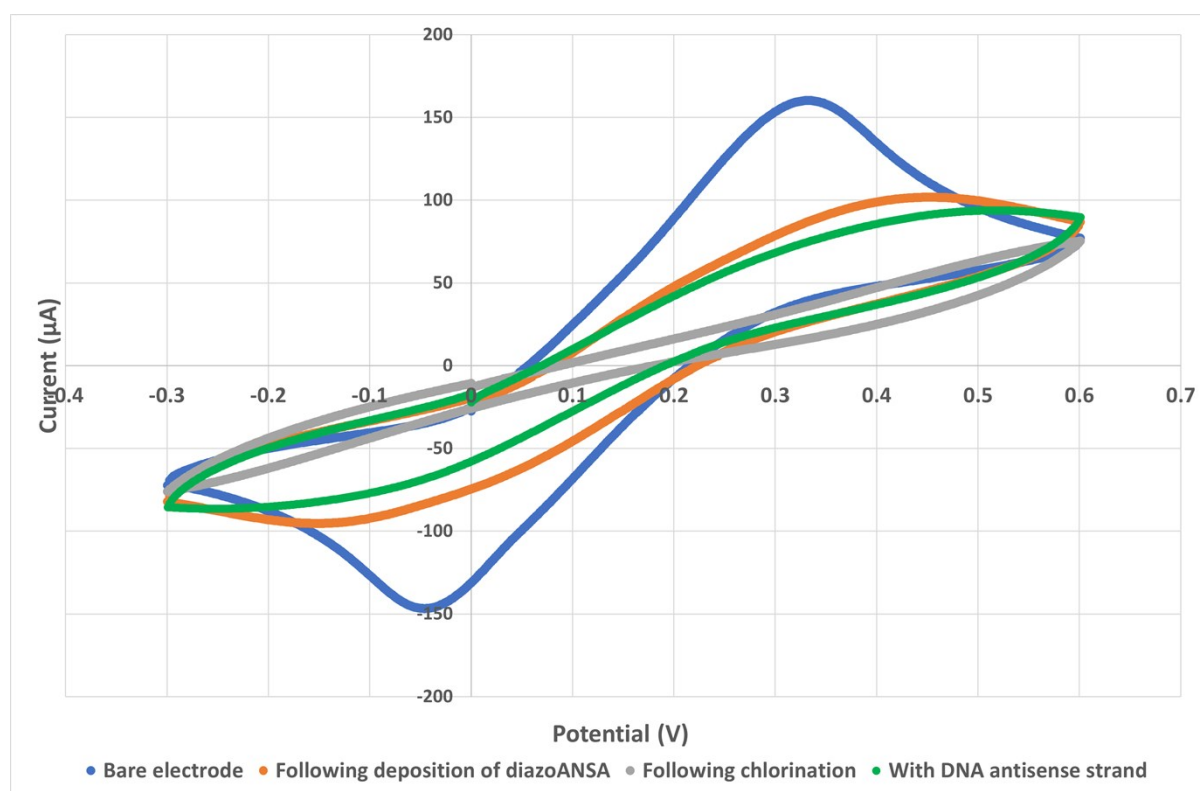


Figure S3: Reductive coulometry changes over fabrication steps.

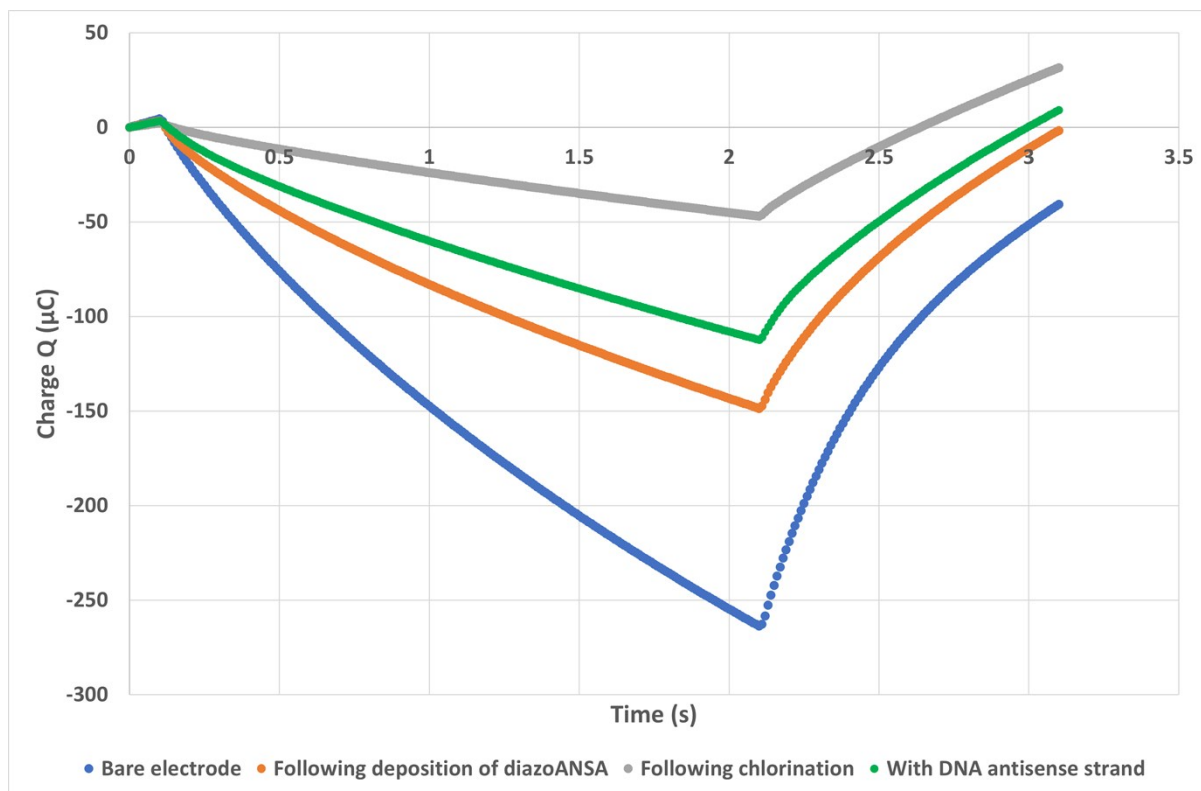


Figure S4: Oxidative coulometry changes over fabrication steps.

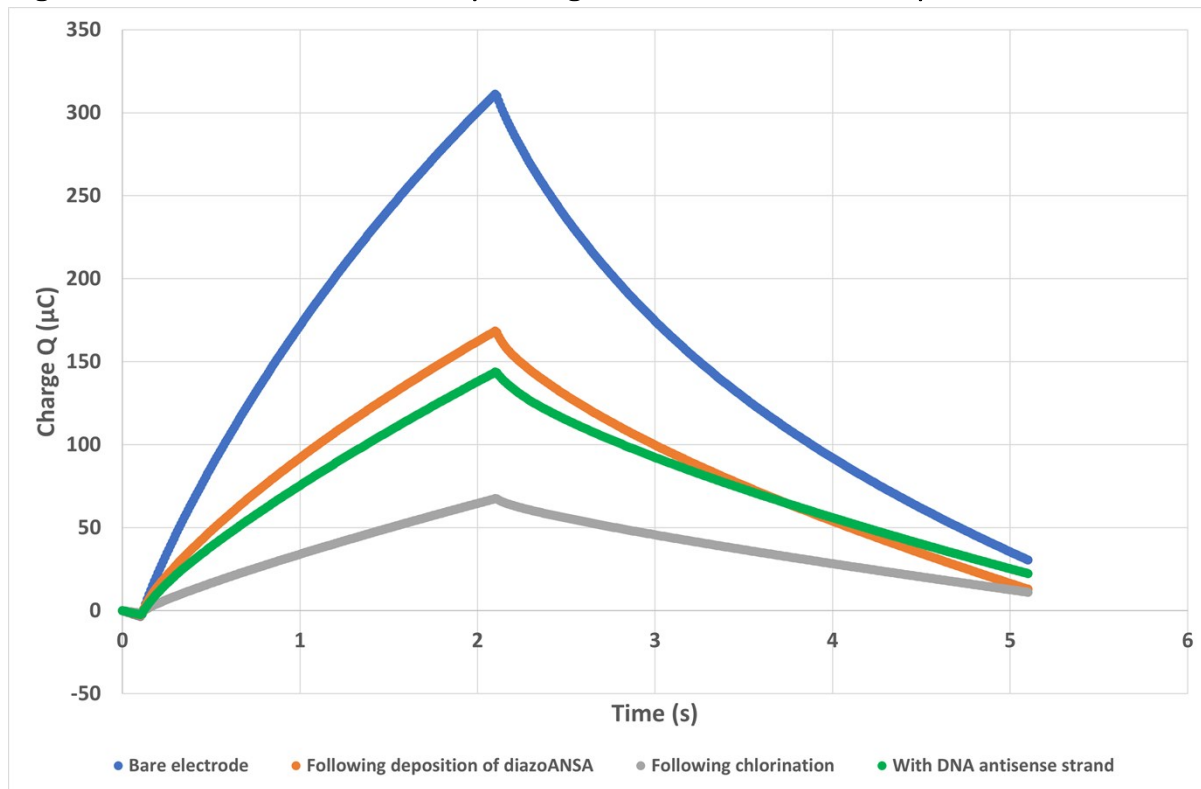


Figure S5: CV deposition cycles.

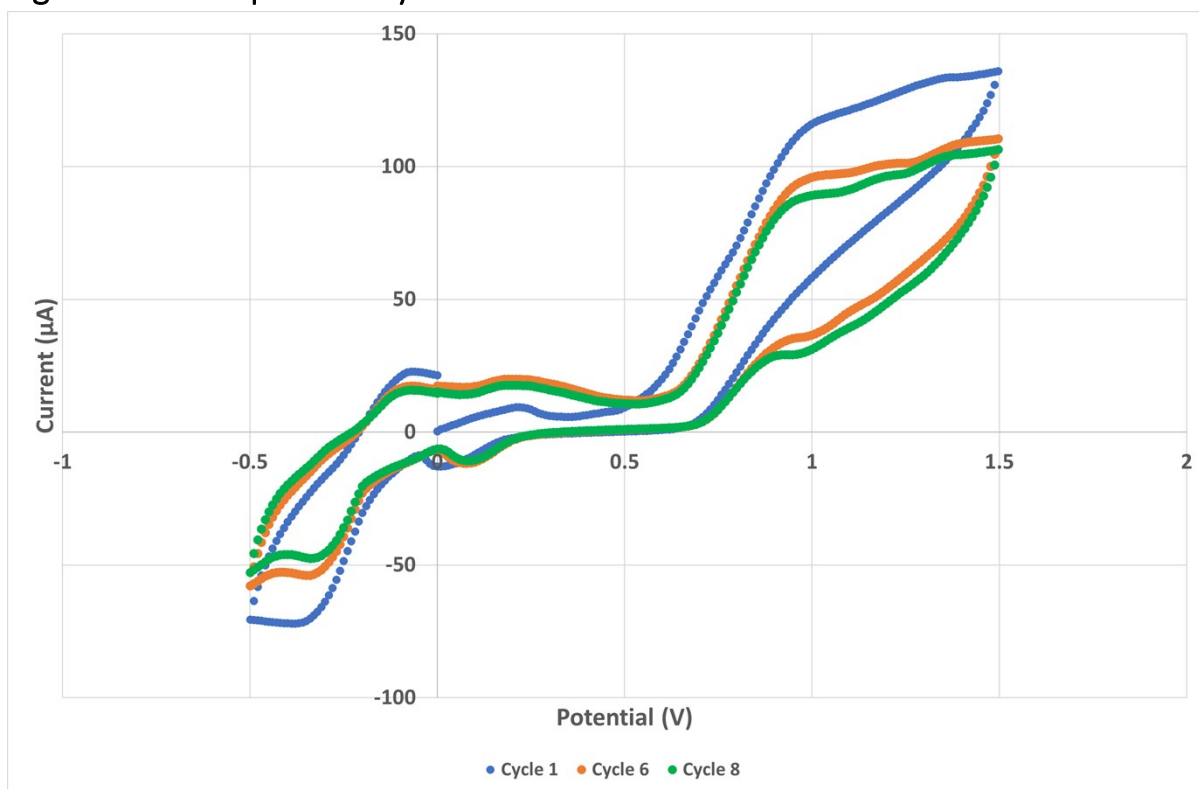


Figure S6: Example oxidative coulometry response following hybridisation with decreasing concentrations of miR-21.

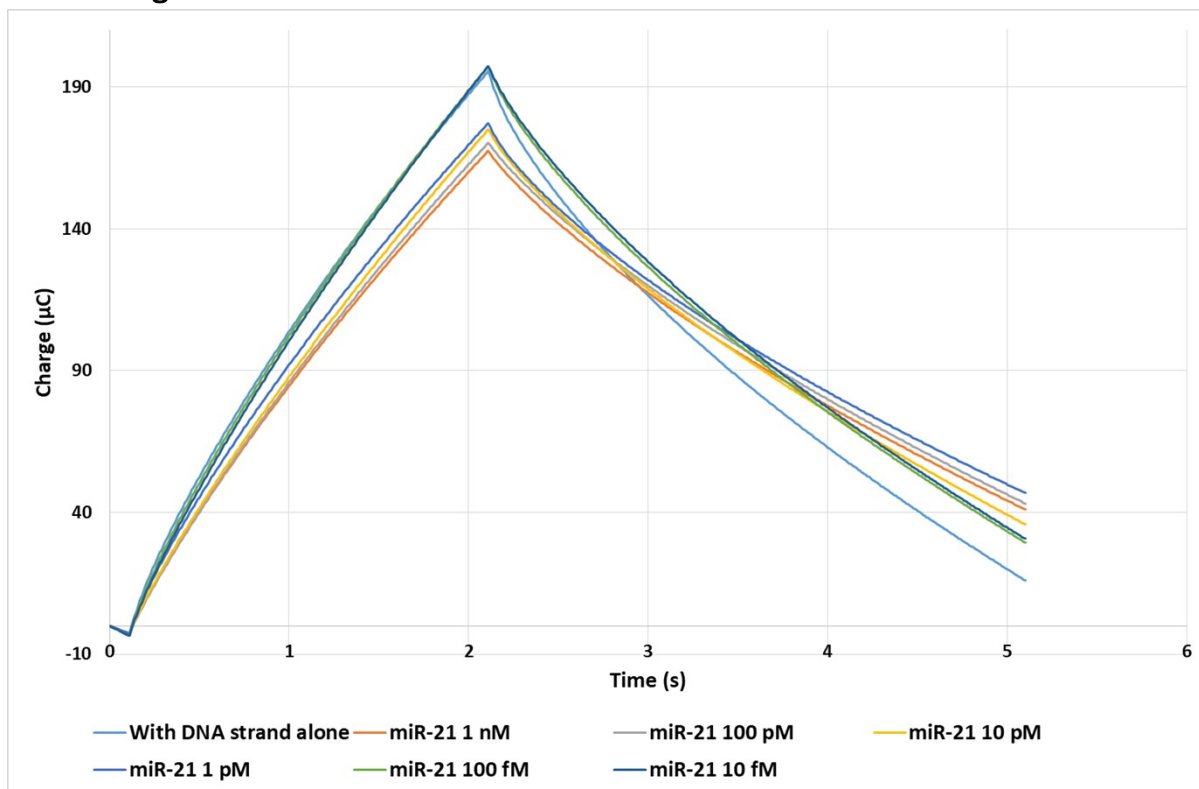


Figure S7: Oxidative coulometry calibration plot for miR-21. Data are expressed as mean +/- SEM (n = 11).

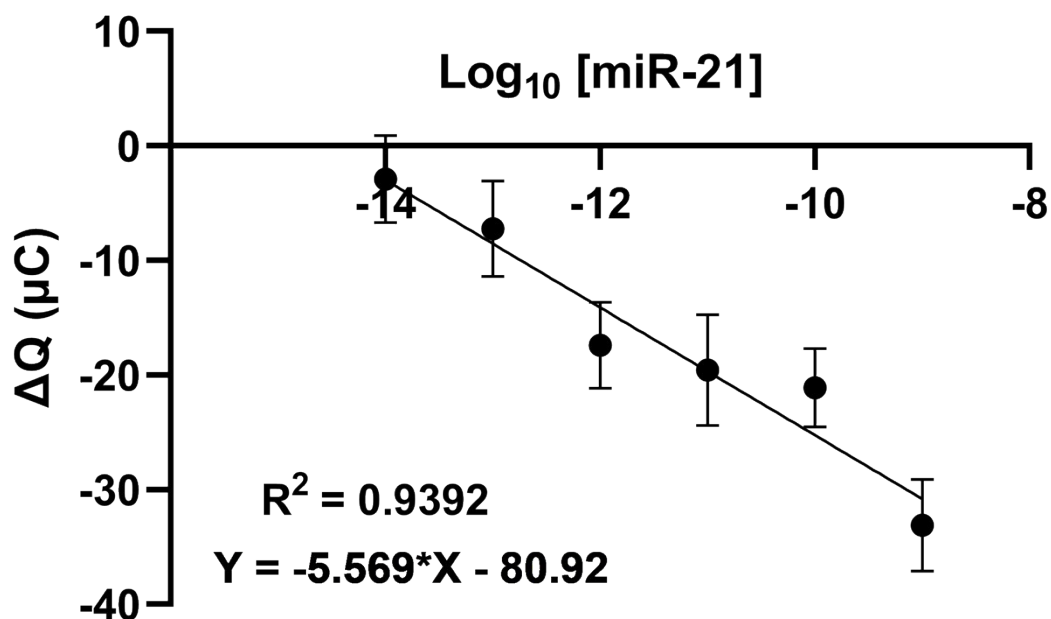


Figure S8: Example differential pulse voltammetry (DPV) response following hybridisation with decreasing concentrations of miR-21.

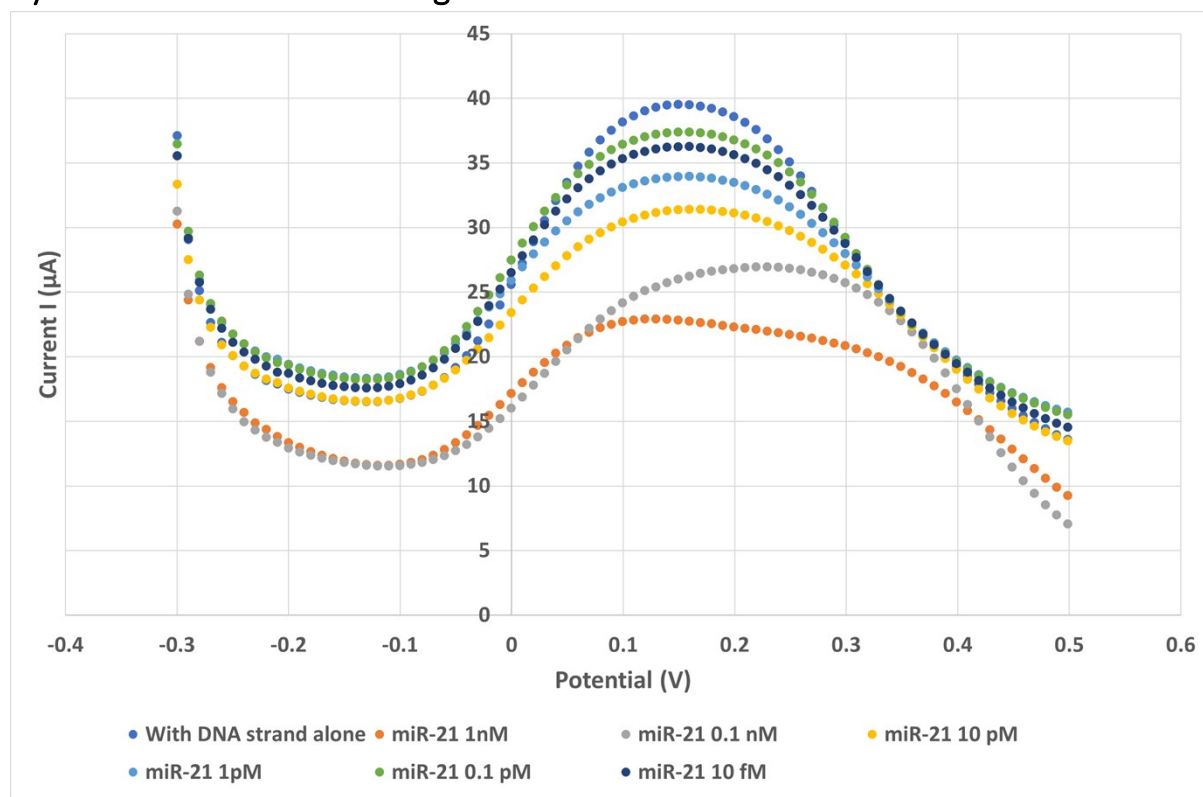


Figure S9: Differential pulse voltammetry (DPV) calibration plot for miR-21. Data are expressed as mean +/- SEM (n = 11).

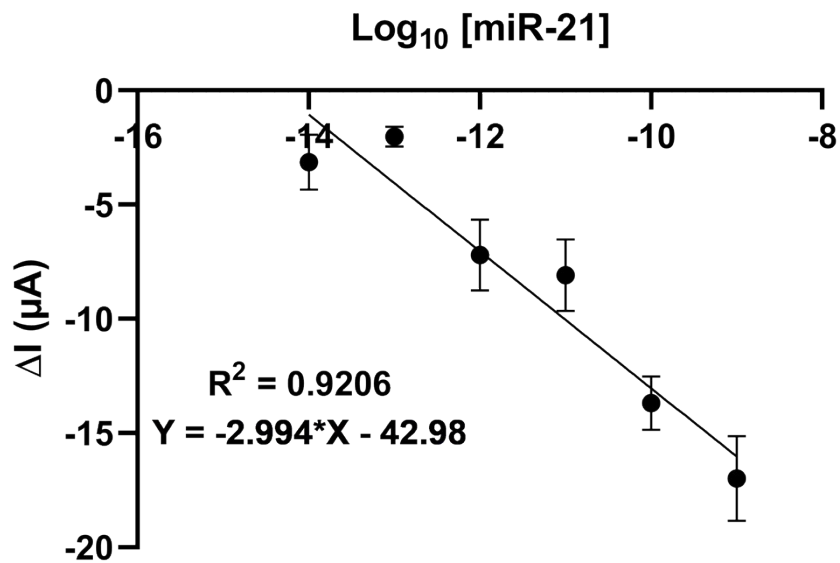


Figure S10: Oxidative coulometry (Echem) and RT-qPCR (PCR) analysis of urinary miR-192 in DKD patients and control subjects. Data were normalised to miR-191 and are expressed as mean as +/- SEM (n = 6 each group). \* = P < 0.05.

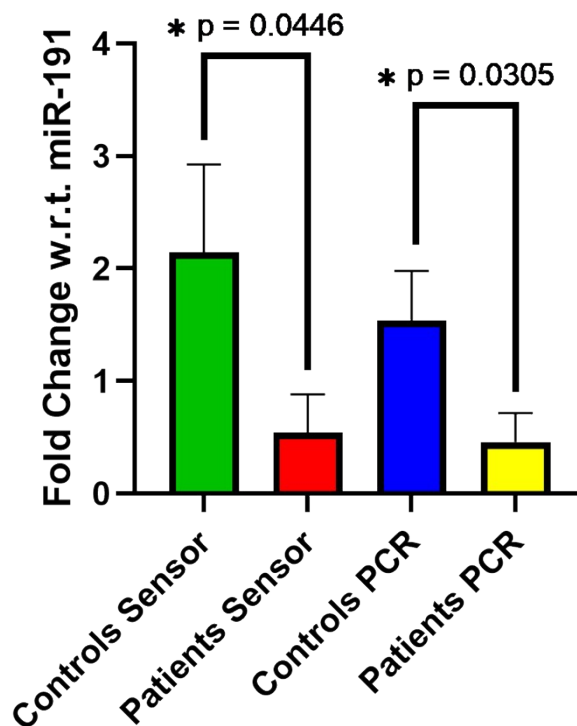


Figure S11: Reductive coulometry analysis of miR-21 in serial dilutions (1/10<sup>th</sup>, 1/50<sup>th</sup>, 1/100<sup>th</sup>, 1/500<sup>th</sup>, 1/1000<sup>th</sup>, 1/5000<sup>th</sup>) of control urine following proteinase K treatment. Data are expressed as mean +/- SEM (n = 3).

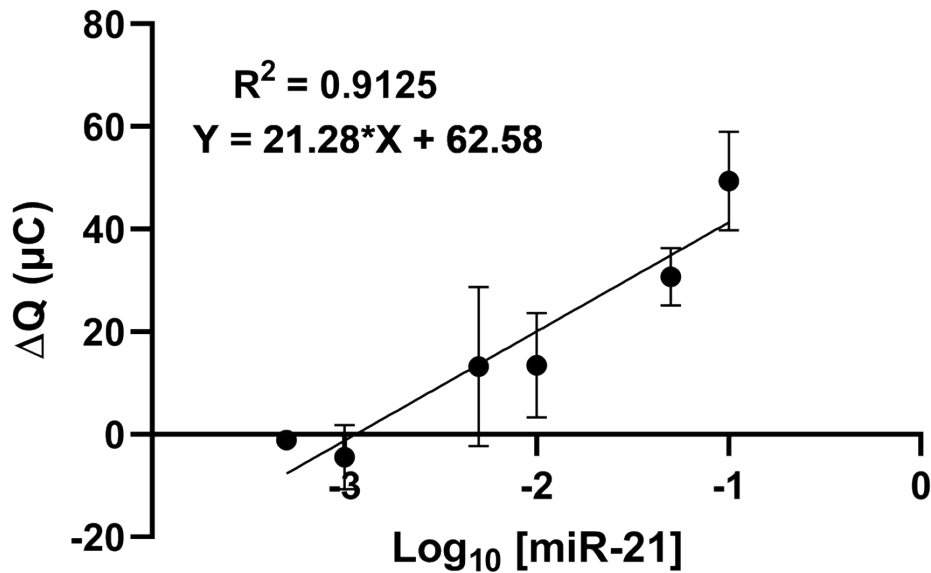


Figure S12: Reductive coulometry measurements investigating uric acid interference, uric acid solutions without miR-21 in blue followed by addition of 10<sup>-11</sup> M miR-21. Data are expressed as mean +/- SEM (n = 3).

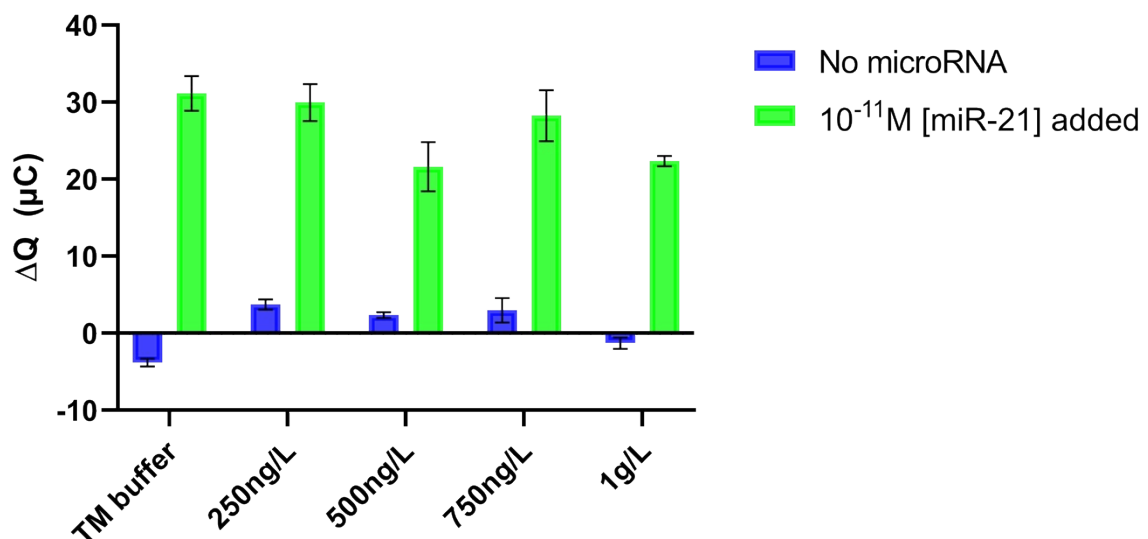


Figure S13: Oxidative coulometry measurements investigating uric acid interference, uric acid solutions without miR-21 in blue followed by addition of  $10^{-11}$  M miR-21. Data are expressed as mean  $\pm$  SEM (n = 3).

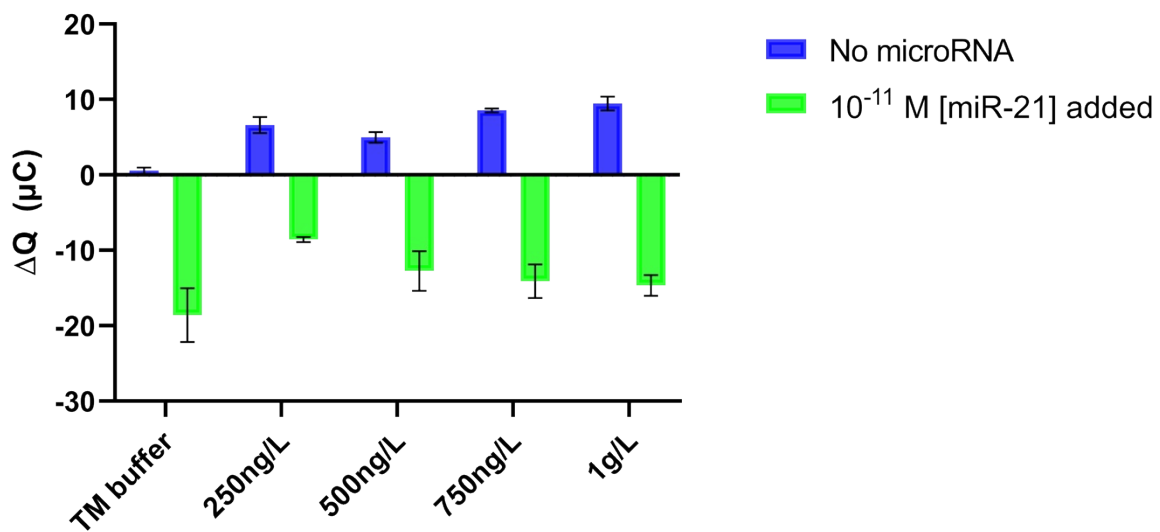
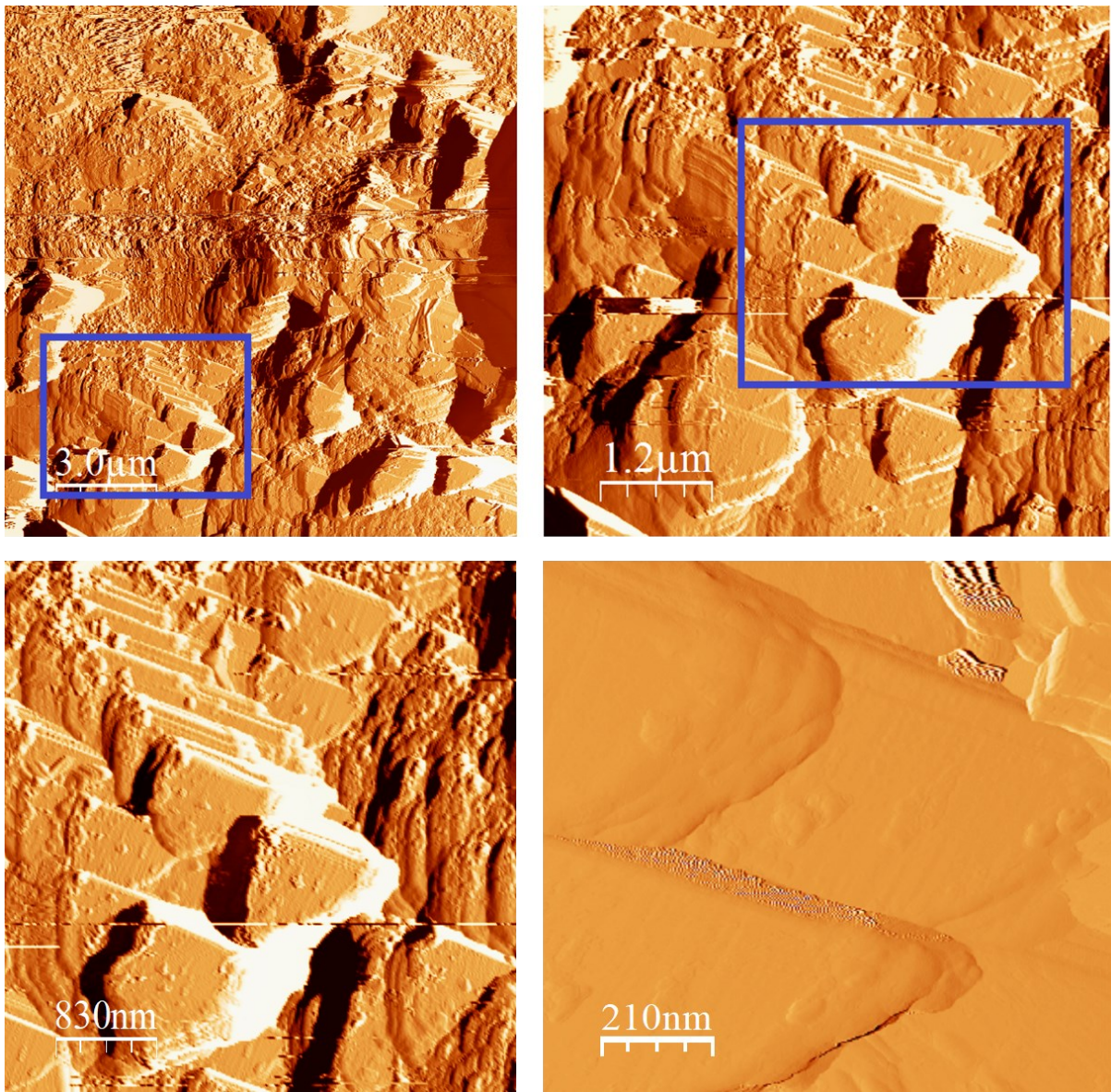
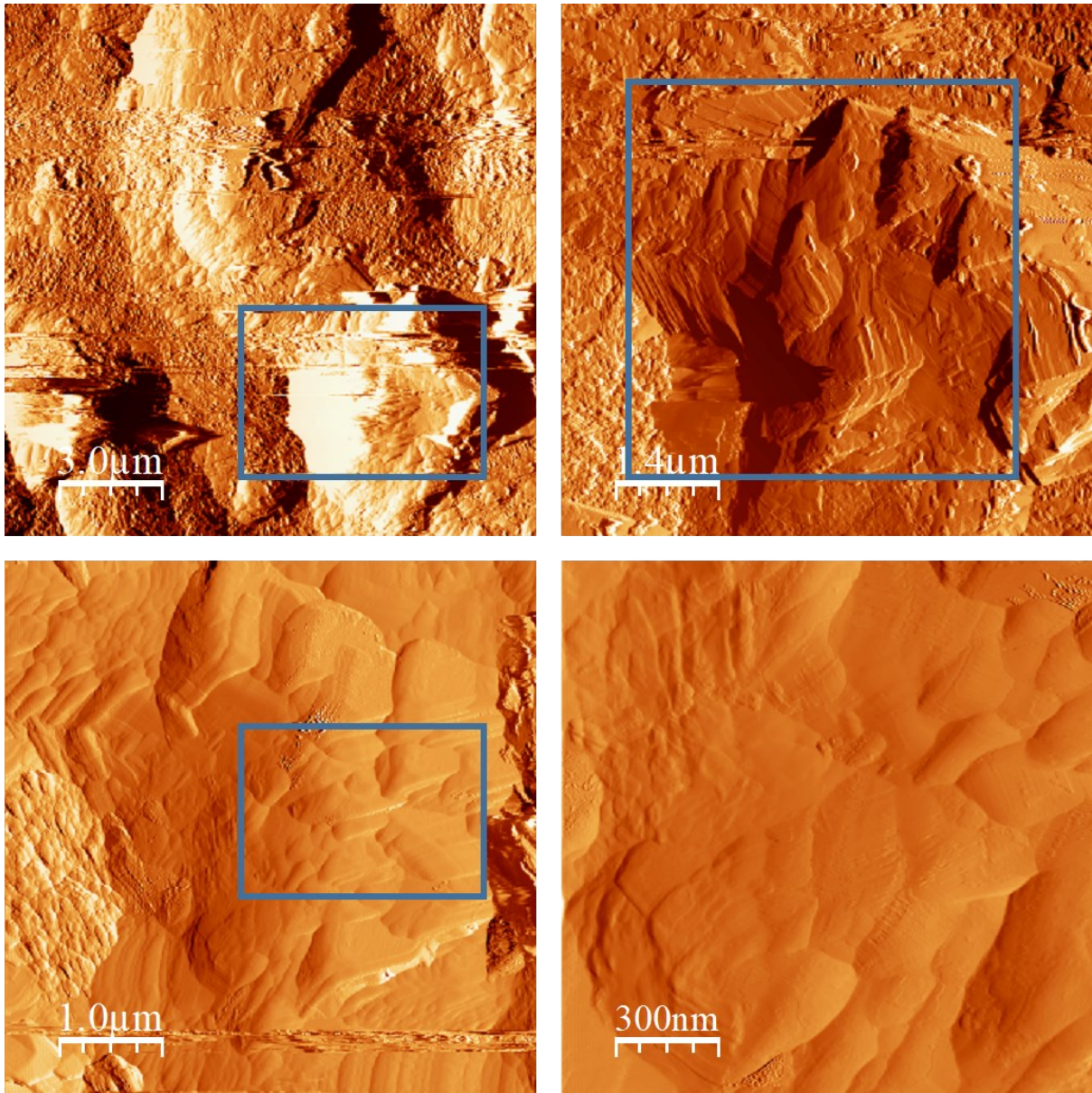




Figure S14: Additional TM-AFM images captured during SPCE modification.



*Fig. S14-1 TM-AFM images of untreated SPCE surface, blue boxes highlight areas of increased magnification.*



*Fig. S14-2 TM-AFM images of the SPCE surface following ANSA deposition, blue boxes highlight areas of increased magnification.*

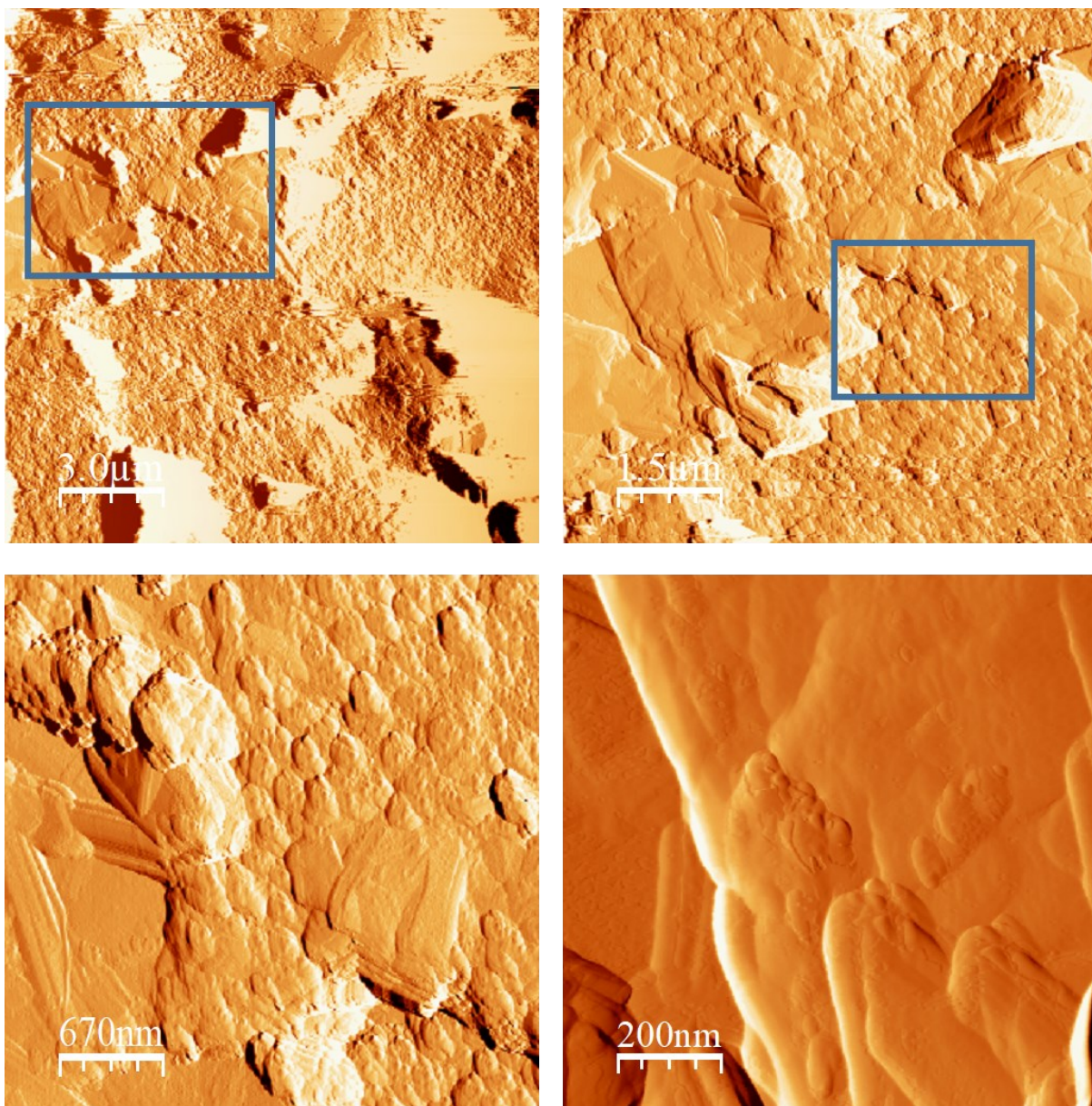


*Fig. S14-3 TM-AFM images of the SPCE surface following DNA oligonucleotide attachment, blue boxes highlight areas of increased magnification.*

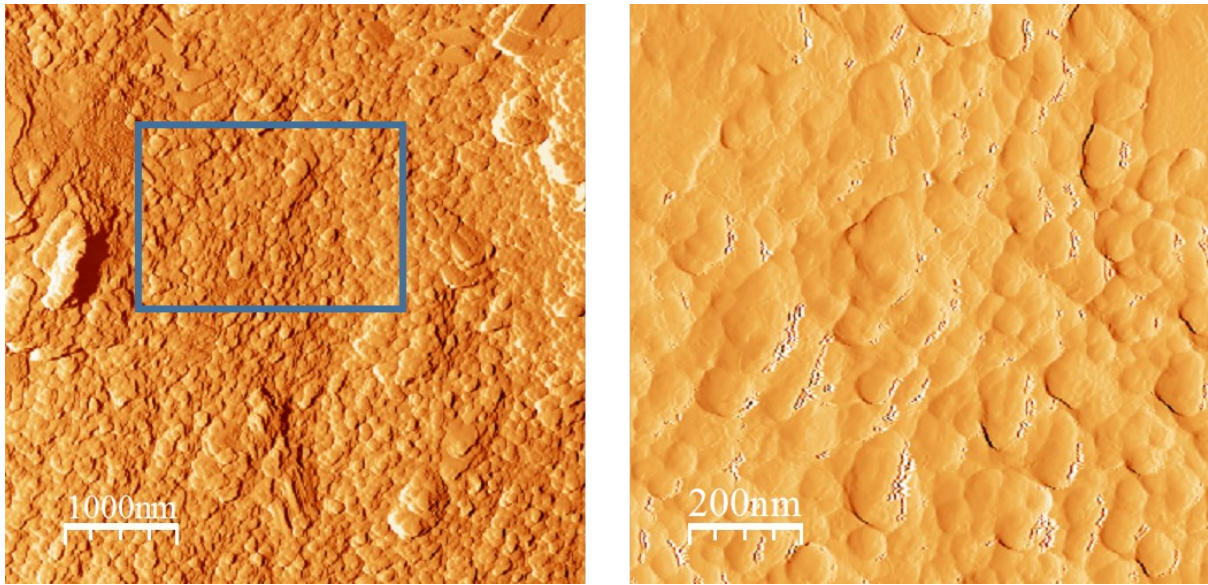


*Fig. S14-4 TM-AFM images of the SPCE biosensor surface following miRNA hybridisation, blue box highlights area of increased magnification.*

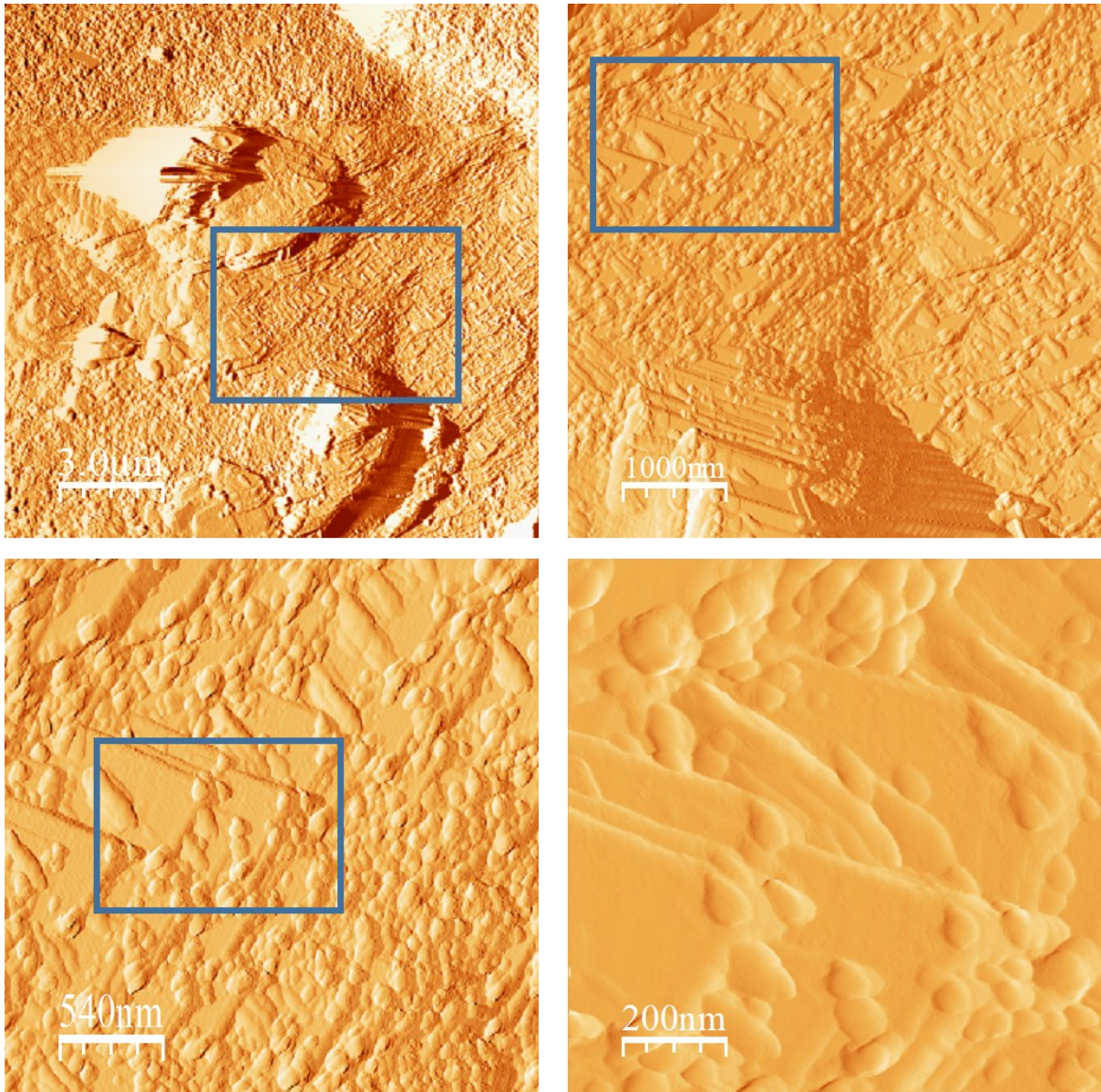


*Fig. S14-5 TM-AFM images of the SPCE biosensor surface following exposure to unprocessed urine, blue boxes highlight areas of increased magnification.*

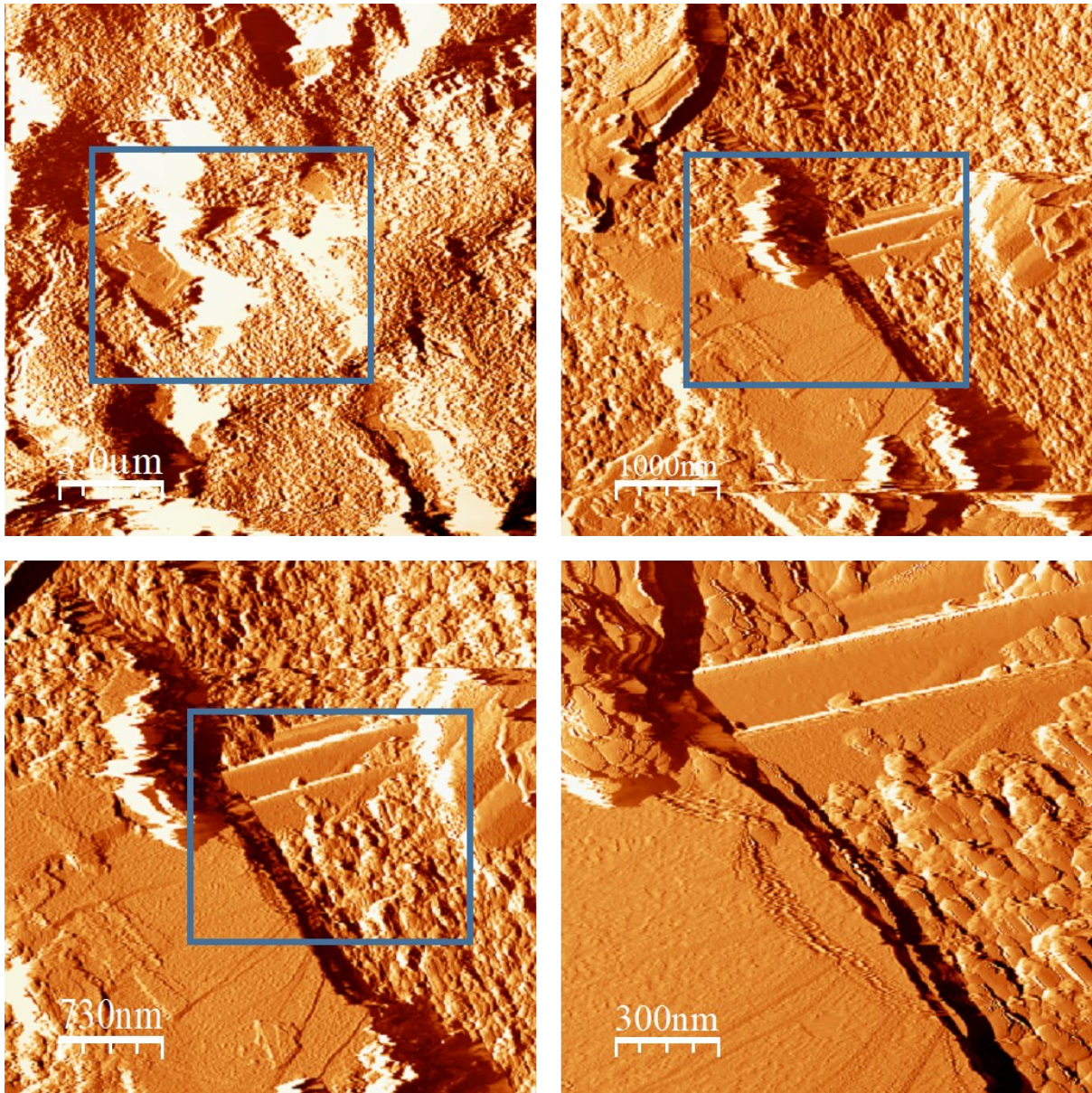


*Figure S14-6 TM-AFM images of the SPCE biosensor surface following exposure to proteinase K treated urine, blue boxes highlight areas of increased magnification.*